II ECCOMAS THEMATIC CONFERENCE ON SMART STRUCTURES AND MATERIALS
C.A. Mota Soares *et al.* (Eds.)
Lisbon, Portugal, July 18-21, 2005

IMPLEMENTATION OF AN ACTIVE DAMPING SYSTEM TO REDUCE HARMONIC VIBRATIONS IN A 3DOF PHYSICAL MODEL

Carlos Moutinho[*], Álvaro Cunha[*] and Elsa Caetano[*]

[*] Faculty of Engineering of University of Porto (FEUP)
R. Dr. Roberto Frias, 4200-465 Porto, Portugal
e-mail: moutinho@fe.up.pt, web page: http://www.fe.up.pt/vibest/

Keywords: Active damping, active mass damper, root-locus design

Abstract. *This paper describes the work for a real implementation of an active damping system to reduce harmonic vibrations in a plane frame physical model with 3 degrees-of-freedom. For this purpose, it is suggested the use of an active mass damper commanded by a derivate controller which has the effect of increasing the modal damping coefficients in correspondence with a specific gain value. This control gain, as well as the system stability, was evaluated using the root-locus technique. The efficiency of the proposed control system to achieve pre-defined damping ratios was verified experimentally, by analyzing the free decay responses of the system after being excited at resonant frequencies.*

1 INTRODUCTION

Many Civil Engineering structures have vibration problems in terms of serviceability limit states due to several transient or periodic dynamic loads, e.g., footbridges subjected to pedestrians actions, road and railway bridges excited by traffic loads and tall building exposed to wind loads.

In these situations, the implementation of control systems can improve the structural performance by reducing the vibration levels to acceptable values, defined for each case. To achieve this, several control devices can be used to apply forces to the structure, calculated by a specific control algorithm.

This study is addressed to practical cases where the dynamic system response is dominated by the contribution of the harmonic vibration of some modes of the structure. In these situations, the amplitude of the response is strongly influenced by the respective damping ratios, meaning that an appropriate control strategy should be able to increase

these damping ratios to predefined values capable to keep the maximum structural response bellow certain limits.

The derivate control, also known as direct velocity feedback control, associated with root locus techniques constitutes a good strategy that can be used for this purpose, since it has the ability to add damping to the structure while providing necessary robustness to the control system[2]. In fact, when some control schemes using collocated pairs of actuators and sensors are used, this strategy leads to unconditionally stable control systems and avoids spillover errors due to unmodeled higher frequency modes. However, when an active mass damper (AMD) is used with this strategy, the control system is no longer unconditionally stable and it may destabilize, particularly for high gains[5].

In this context, the objective of this work is to implement an active control system to increase the damping ratios in a 3DOF plane frame physical model. To achieve this goal, an AMD was installed in the top floor of the model, the control force being calculated based on the derivate control law.

To verify the proposed control system efficiency, the model is excited by several harmonic loads induced by a small shaking table, and the system response is analyzed in terms of the damping ratios achieved, as well as the control system stability.

2 DYNAMIC MODELING OF MECHANICAL SYSTEMS

2.1 Equations of motion

Consider the system indicated in the Figure 1 which represents a 2-DOF shear building structure composed by the masses m, connected through 2 levels of columns with total stiffness k and 2 linear viscous dampers with damping constant c, subjected to the time dependent forces f_1 and f_2.

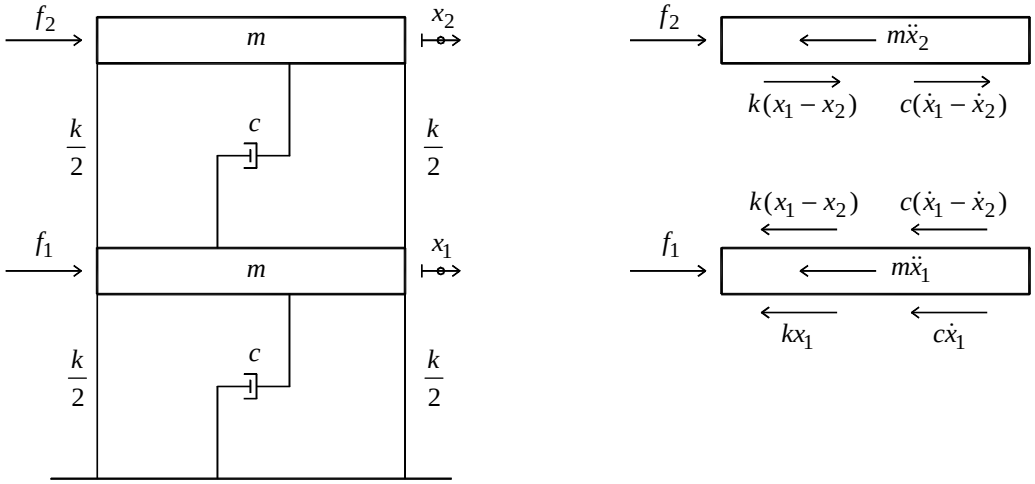

Figure 1: 2-DOF shear building structure and the respective free body diagrams

The free body diagrams of the 2 masses of the system allow to establish the following equations of motion

$$\begin{aligned} m\ddot{x}_1 + c\dot{x}_1 + c(\dot{x}_1 - \dot{x}_2) + kx_1 + k(x_1 - x_2) &= f_1 \\ m\ddot{x}_2 - c(\dot{x}_1 - \dot{x}_2) - k(x_1 - x_2) &= f_2 \end{aligned} \tag{1}$$

These equations can be written in the matrix form

$$\begin{bmatrix} m & 0 \\ 0 & m \end{bmatrix} \begin{Bmatrix} \ddot{x}_1 \\ \ddot{x}_2 \end{Bmatrix} + \begin{bmatrix} 2c & -c \\ -c & c \end{bmatrix} \begin{Bmatrix} \dot{x}_1 \\ \dot{x}_2 \end{Bmatrix} + \begin{bmatrix} 2k & -k \\ -k & k \end{bmatrix} \begin{Bmatrix} x_1 \\ x_2 \end{Bmatrix} = \begin{Bmatrix} f_1 \\ f_2 \end{Bmatrix} \tag{2}$$

or simply

$$M\ddot{x} + C\dot{x} + Kx = f \tag{3}$$

where M, C and K are the mass, damping and stiffness matrices, respectively, $\ddot{x}$, $\dot{x}$ and x are the accelerations, velocities and displacements vectors, and f is the loads vector.

In the general case of a n-DOF structure, the system of n coupled second order differential equations (3) can be alternatively described, under the assumption of proportional damping, by a set of n independent differential equations by means of a transformation of the physical coordinates x to modal coordinates z according to[1]

$$x = \Phi z \tag{4}$$

where Φ is the modal matrix which contains the vectors of the n vibrations modes of the structure $\phi_1, \phi_2, \ldots, \phi_n$. These vibrations modes are in correspondence with the n undamped natural circular frequencies of the system $\omega_1, \omega_2, \ldots, \omega_n$, and verify the well-known orthogonality conditions.

The substitution of eq.(4) into eq.(3) and the application of the orthogonality relationships leads to the following independent differential equations

$$m_i\ddot{z}_i + c_i\dot{z}_i + k_i z_i = f_i \tag{5}$$

with the notations

$$m_i = \phi_i^T M \phi_i \;;\; c_i = \phi_i^T C \phi_i \;;\; k_i = \phi_i^T K \phi_i \tag{6}$$

m_i, c_i and k_i are the modal mass, modal damping coefficient and modal stiffness in correspondence with the i^{th} vibration mode of the structure.

2.2 System Transfer Functions

Taking the Laplace transform of both sides of eq.(2), after setting initial conditions to zero, one obtains[3]

$$\begin{bmatrix} ms^2 + 2cs + 2k & -cs - k \\ -cs - k & ms^2 + cs + k \end{bmatrix} \begin{Bmatrix} X_1(s) \\ X_2(s) \end{Bmatrix} = \begin{Bmatrix} F_1(s) \\ F_2(s) \end{Bmatrix} \tag{7}$$

Solving this system of equations in order to obtain $X_1(s)$ and $X_2(s)$, yields

$$X_1(s) = \frac{ms^2 + cs + k}{m^2s^4 + 3cms^3 + (c^2 + 3km)s^2 + 2cks + k^2} F_1(s) + \frac{cs + k}{m^2s^4 + 3cms^3 + (c^2 + 3km)s^2 + 2cks + k^2} F_2(s)$$

$$X_2(s) = \frac{cs + k}{m^2s^4 + 3cms^3 + (c^2 + 3km)s^2 + 2cks + k^2} F_1(s) + \frac{ms^2 + 2cs + 2k}{m^2s^4 + 3cms^3 + (c^2 + 3km)s^2 + 2cks + k^2} F_2(s) \tag{8}$$

Each system input-output relation is in correspondence with a transfer function that establishes, in the Laplace variable domain, the deterministic relationship between that input and output. In general, for a MIMO system with *p* inputs and *q* outputs there are a total of $p \times q$ transfer functions which can be grouped in a single matrix called transfer function matrix.

In the example of the structure of Fig.1, there are two inputs and two outputs which mean that there are four transfer functions, $G_{11}(s)$, $G_{12}(s)$, $G_{21}(s)$ and $G_{22}(s)$, with the corresponding transfer function matrix

$$G(s) = \begin{bmatrix} G_{11}(s) & G_{12}(s) \\ G_{21}(s) & G_{22}(s) \end{bmatrix} \tag{9}$$

More specifically, these transfer functions can be defined as follows

$$G_{11}(s) = \left.\frac{X_1(s)}{F_1(s)}\right|_{F_2(s)=0} , \; G_{12}(s) = \left.\frac{X_1(s)}{F_2(s)}\right|_{F_1(s)=0}$$

$$G_{21}(s) = \left.\frac{X_2(s)}{F_1(s)}\right|_{F_2(s)=0} , \; G_{22}(s) = \left.\frac{X_2(s)}{F_2(s)}\right|_{F_1(s)=0} \tag{10}$$

Combining eq.(10) with eq.(8), one can obtain the following transfer function matrix

$$G(s) = \begin{bmatrix} \dfrac{ms^2 + cs + k}{m^2s^4 + 3cms^3 + (c^2 + 3km)s^2 + 2cks + k^2} & \dfrac{cs + k}{m^2s^4 + 3cms^3 + (c^2 + 3km)s^2 + 2cks + k^2} \\ \dfrac{cs + k}{m^2s^4 + 3cms^3 + (c^2 + 3km)s^2 + 2cks + k^2} & \dfrac{ms^2 + 2cs + 2k}{m^2s^4 + 3cms^3 + (c^2 + 3km)s^2 + 2cks + k^2} \end{bmatrix} \tag{11}$$

In the general case of a *n*-DOF structure, the transfer function matrix can be obtained directly using the system matrices *M*, *C* and *K*, according to

$$G(s) = \left[Ms^2 + Cs + K\right]^{-1} \tag{12}$$

If the system has several degrees-of-freedom, the analytical determination of the system transfer functions can be very laborious using eq.(12). In this case, these transfer functions can be alternatively obtained using the modal decomposition method mentioned in the previous section. With this technique, it is possible to define a simplified model of

the system, considering only the contribution of the first n vibrations modes of the structure. The corresponding transfer function matrix is then given by

$$G(s) = \sum_{i=1}^{n} \frac{\phi_i \phi_i^T}{m_i (s^2 + 2\zeta_i \omega_i s + \omega_i^2)} \tag{13}$$

where ω_i is the undamped natural circular frequency of the i^{th} vibration mode of the structure, ϕ_i is the respective mode shape vector, and m_i and $\zeta_i = c_i / 2m_i\omega_i$ are the corresponding modal mass and modal damping ratio, respectively.

2.3 Analysis of system poles and zeros

One of the most significant advantages of defining a system model by its transfer functions using Laplace transform is that it allows to develop graphical techniques for predicting the system performance without actually solving the system of differential equations[4]. In fact, the analysis of these transfer functions allows to obtain the location of the poles and zeros of the system, which gives sufficient information about the quality of the system response to several kind of inputs.

The typical form of a transfer function of the system is

$$G(s) = a \frac{\prod (s - z_i)}{\prod (s - p_i)} \tag{14}$$

where a is a real constant, and p_i and z_i are the poles and the zeros of the transfer function, respectively.

The poles are the values of the Laplace transform variable, s, for which the denominator of the transfer function becomes zero. These poles are related with the natural frequencies and damping ratios of the system. Because any transfer function of the system reflects the system properties, all the system transfer functions have necessarily the same denominator. In an ordinary underdamped structure, each natural frequency frequency ω_i and damping coefficient ζ_i are in correspondence with a pair of poles, according to[4]

$$p_i = -\zeta_i \omega_i \pm j\omega_i \sqrt{1 - \zeta_i^2} = -\zeta_i \omega_i \pm j\omega_{d,i} \tag{15}$$

where $\omega_{d,i}$ denotes the corresponding damped circular frequency. Figure 2 represents graphically, in the s-plane, the location of poles given by the previous equation.

It can be readily seen that, if the system poles are plotted in a figure, qualitative information about that system can be immediately extracted by just observing the poles location. For example, if the poles are located in the imaginary axis that means that the system has no damping. On the other hand, if the poles are far way from the imaginary axis, the system is damped.

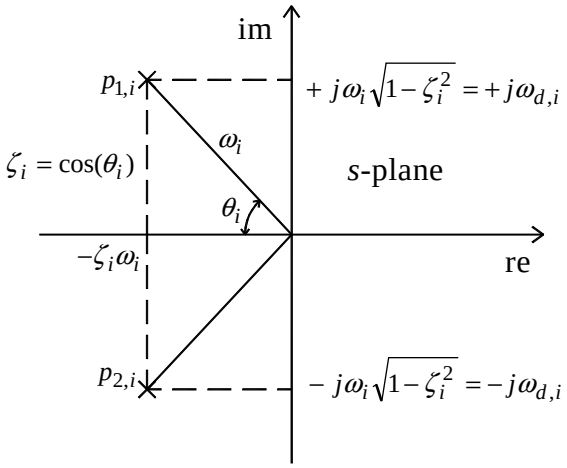

Figure 2: Pole diagram for an underdamped system

On the other hand, the zeros are the values of the Laplace transform variable, *s*, for which the numerator of the transfer function becomes zero. In an ordinary structure, the zeros of the transfer function are related with the excitation frequencies which minimize the response at the degree-of-freedom where the response is measured. In structural dynamics, these frequencies are called anti-resonance frequencies. In contrast to the poles, the zeros may be different for the several transfer functions of the structure.

2.4 Systems with collocated and non-collocated actuator and sensor

In a structure, if the actuator and sensor are positioned at the same point, it is said that the system is collocated, otherwise the system is non-collocated. Figure 3 represents the pole and zero plot of a system transfer function where the actuator and sensor are collocated and non-collocated (only the upper half of complex plane is represented because this diagram is symmetric with respect to the real axis). In the collocated case, the transfer function has alternating imaginary poles and zeros. This doesn't happen in the non-collocated case. As discussed in the next sections, the alternating pole and zero property is very important in the area of control systems, because it guaranties stability robustness in a wide class of single-input single-output (SISO) systems[2].

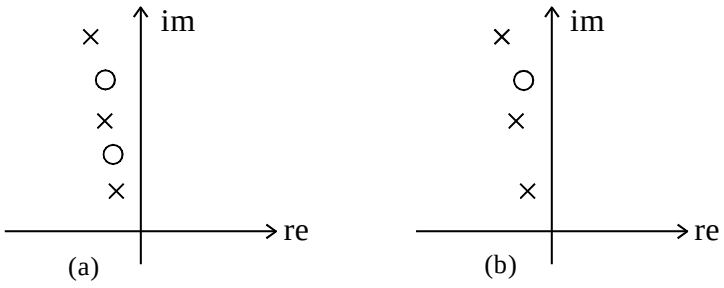

Figure 3: Pole and zero plots for a system with (a) collocated and (b) non-collocated actuator/sensor

3 DESIGN OF CONTROL SYSTEMS BY THE ROOT-LOCUS METHOD

3.1 Close-loop and Open-loop transfer functions

Consider the block diagram indicated in Figure 4, which represents a close-loop negative feedback system. The output $X(s)$ is fed back into the system $G(s)$ after being multiplied by $H(s)$.

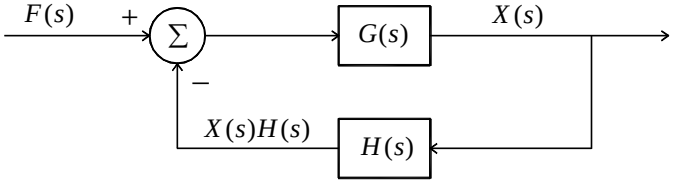

Figure 4: Block diagram of a close-loop negative feedback system

The overall transfer function that relates the Laplace transform of the input and output of the compensated system is known as the closed-loop transfer function and is given by[4]

$$\frac{X(s)}{F(s)} = \frac{G(s)}{1 + H(s)G(s)} \tag{16}$$

The product $H(s)G(s)$ is known as the open-loop transfer function. It is obvious that the choice of the compensator $H(s)$ is important to define the behavior of the controlled system. In fact, its response is influenced by the location of the poles and zeros of the close-loop transfer function, which are conditioned by the type of the chosen compensator. It is now clear that an ideal compensator should be able to modify the poles and zeros location in such way that its values can become in correspondence with select system response parameters.

3.2 System compensation with derivate control

One type of compensator that can be used in system control is the derivate control. This compensator is a particularization of the proportion-integral-derivate (PID) control when only the derivate component is considered. The derivate control, also known as velocity feedback control, adds damping into the system and thus provides stability[2].

This compensator generates a control force which is proportional to the derivate of the system response, i.e., the system velocity. The effect achieved is similar to attaching a viscous damper to a structure. The transfer function of such compensator is

$$H(s) = ks \tag{17}$$

where k is a real constant and s is the Laplace transform variable. The k value is related with the ratio of velocity applied to the system, which is in correspondence with the damping coefficient of the equivalent damper mentioned before.

3.3 Root-locus analysis

As mentioned before, the poles of a transfer function of a second order system are related with the respective natural frequencies and damping ratios, which gives sufficient information about the quality of the system response to several kinds of inputs. This concept is the basis of the root-locus diagram of a controlled system, because the knowledge of the poles of the closed-loop transfer function provides information about how the original system is modified with the control action.

The root-locus is the locus of the poles (or the roots of the denominator) of the closed-loop transfer function $1+gH(s)G(s)$ when the real positive parameter g, called gain, varies from zero to infinity. The modification of the gain associated with the compensator changes the poles location of the system to other positions in such a way that a path can be drawn corresponding to several levels of gain.

Figure 5 represents the upper half of the root-locus plot of a controlled structure like the one represented in Figure 1, where the system input-output refers to the same point (i.e., the actuator and sensor are collocated) and compensator is a derivate controller.

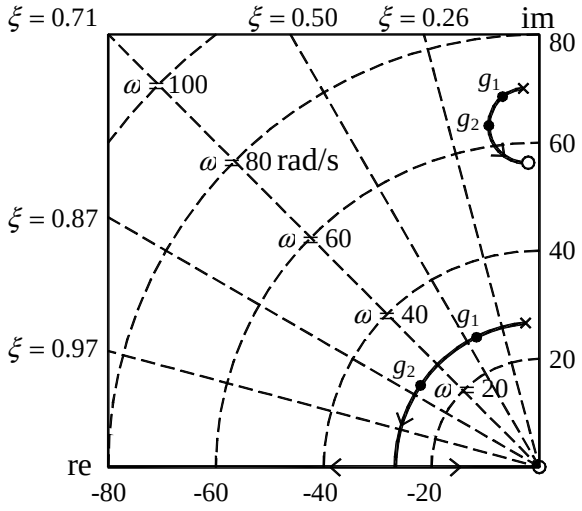

Figure 5: Root-locus diagram for collocated derivate control

This graphical method is a powerful tool in the analysis and design of control systems, because the modification of the poles location caused by a gain adjustment suggests which value of gain should be chosen to meet some system response specifications.

The sketch the root-locus diagram can be very easy if some rules are observed. For example, the close-loop poles of the system goes from the open-loop poles to the open-loop zeros as the gain increases from zero to infinity[4].

The root-locus method has another useful advantage because it allows to analyze the system stability when using different compensators, control schemes or gain levels. In stability analysis, it is demanded that the close-loop poles remain at the left side of the imaginary axis because it guaranties positive damping in all vibration frequencies.

3.4 Collocated versus non-collocated control

In section 2.4 it was seen that when the actuator and sensor are collocated the respective transfer function has alternating imaginary poles and zeros. It doesn't happen in the non-collocated case. The location of poles and zeros and the relation between their positions is very important when studying a control system[2].

Figure 6 represents a typical aspect of the upper half root-locus diagram of a controlled structure with several degrees-of-freedom, for the collocated and non-collocated sensor/actuator case. The compensator is a derivate controller which has the effect of adding a zero in the open-loop transfer function (represented at the origin of the real/imaginary axis).

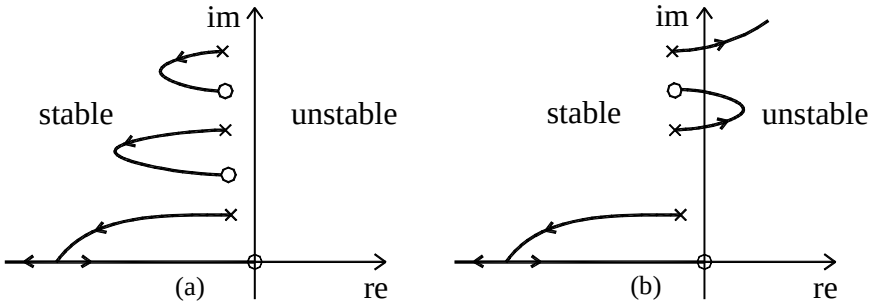

Figure 6: Root-locus diagram for (a) collocated and (b) non-collocated derivate control

As said before, the close-loop poles of the controlled system go from the open-loop poles to the open-loop zeros as the gain increases from zero to infinity. Any point *P* of a specific trajectory of the root-locus diagram verifies the following equation[4]

$$\theta = \sum_{i=1}^{n_z} \angle(s + z_i) - \sum_{j=1}^{n_p} \angle(s + p_j) = (2k+1) \times 180^\circ \tag{18}$$

where k = 0, ±1, ±2, ±3…, n_z is the number of zeros, n_p is the number of poles and $\angle(s+z_i)$ and $\angle(s+p_j)$ are the angles of the vectors drawn from the zeros and the poles, respectively, to point *P*. This equation can be used to define departure and arrival angles of the several branches from poles to the zeros.

When collocated control is used, the departure angles of the close-loop poles are all in the same way. As a result, several nice stabilizing loops are generated, which reveals a good performance of this type of control. In fact, even if the system parameters have some level of uncertainty, the root-locus keeps the same general shape and remains entirely within the left half complex plane. Such control system is said to be robust with respect to stability[2].

In contrast, the non-collocated control scheme causes pole-zero flipping and the alternating property is no longer verified. In this case, the departure angles have different ways and the system becomes unstable for a small gain. In this situation, it is desirable that the system has some damping (because it moves the poles to the left side) in order to archive a larger gain margin.

3.5 Control system using an active mass damper

One of the most widely known actuator system for application of control forces in a structure is the active mass damper (AMD). This device generates internal inertial forces in the system without having any external connections. Although this actuation system may be desirable in many practical situations, some design issues must be carefully observed[5].

The first important aspect is that the AMD doesn't correspond to a collocated control scheme. In fact, although the actuator is positioned in the same location as the control point, the force generated with this device is applied at two different locations. Figure 7 represents an example of the application of an AMD to a single degree-of-freedom structure. In this case, the control force is calculated in correspondence with the structure response x_1, but is applied as a pair of forces at the degrees-of-freedom corresponding to x_1 and x_2.

This non-collocated control system is potentially unstable because the close-loop poles may be located at the right side of the imaginary axis of the complex plane, particularly when high gains are used.

To better understand this problem, let's consider a general structure with several degrees-of-freedom. In Figure 8a it is represented the root-locus diagram of a control system composed by an AMD with low frequency and high damping, positioned at the top of a 3-DOF shear building structure. The control point is in correspondence with the actuator location and the compensator is a derivate controller.

The root-locus represents the path of the close-loop poles locations as the gain varies from zero to infinity. In this case, the departure angles of the poles corresponding to the vibrations modes of the structure are directed to the left side and the corresponding branches describe stable loops. In contrast, the close-loop pole corresponding to the AMD mode, departs to the right side, in the direction of the unstable region of the complex plane. As the gain increases, the damping coefficients of the vibration modes of the structure also increase and the damping coefficient of the vibration mode of the AMD decreases. For a specific gain value, the close-loop pole of the AMD intercepts the

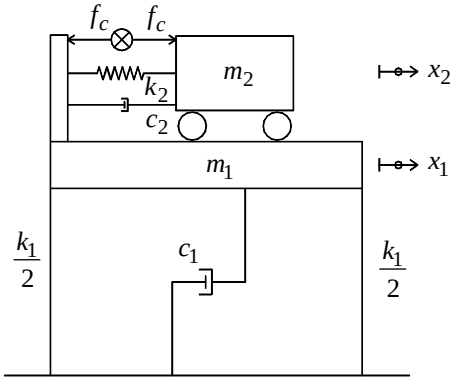

Figure 7: 1-DOF structure with an active mass damper

imaginary axis defining the maximum gain value, g_{max}, from which the control system gets unstable. This value of gain is very important because not only defines the gain that causes system instability, but also establishes the maximum modal damping coefficients achievable with this control scheme.

One important conclusion about the AMD properties can now be understood. In order to get a larger gain margin before instability, the AMD should have a high level of damping, because the path that the respective close-loop pole has to go through until it crosses the imaginary axis, is longer as the damping of this device increases.

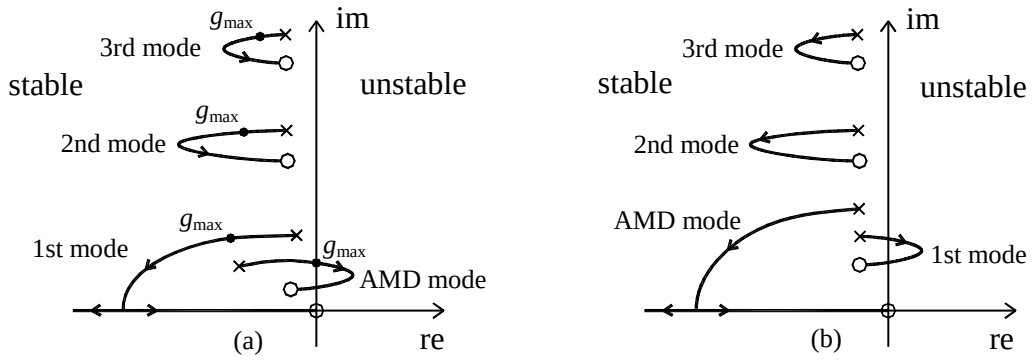

Figure 8: Root-locus diagram of a controlled structure using an AMD with (a) low and (b) high frequency

From Figure 8a, it is clear that if the natural frequency of the AMD is lower than all the natural frequencies of the original structure, the system stability is dependent on the control device properties and, as the gain increases, the original structure gets more damped. This is a good procedure, because the objective of the control is achieved, which is to reduce the behavior of the original structure by increasing its damping. However, the damping of the device decreases which may lead to a big motion of it mass. This is not preoccupant because the active mass works as a parasite mass and, as long as it displacement keeps in an acceptable margin (avoiding shocks with the physical boundaries) it doesn't affect the performance of the structure control.

On the other hand, if the natural frequency of the AMD is greater than the first natural frequency of the original structure, a zero-pole flipping is observed in the intermediate frequencies of the structure (see Figure 8b). This is disastrous because the damping coefficients of the modes with frequencies below the frequency of the AMD decreases as the gain increases. As a consequence, in the root-locus diagram the close-loop poles of these modes have branches with departure angles directed to the unstable region and the AMD branch describes a stable trajectory. If the structure is lightly damped, it is necessary just a small gain to get the system unstable by one of these modes.

As a conclusion, it should be focused that an ideal AMD used to control a structure should have high damping in order to get a larger gain margin and get a more damped structure, and should have a natural frequency below the first natural frequency of the original structure to avoid instability of the lower vibration modes.

4 CHARACTERIZATION OF THE EXPERIMENTAL CONTROL SYSTEM

4.1 Model and equipment description

After understanding the theoretical concepts about how to control a structure using the root-locus method, in order to modify the structural parameters to meet some system response specifications, it was conducted a real implementation of a control system with the objective of reducing harmonic vibrations in a plane frame physical model. For this purpose, it was developed a model of a shear building structure with 3 floors and an active mass damper to control vibrations, both shown in Figures 9a and 9b.

The physical model is composed by 3 rigid iron masses connected to each other and to the base through aluminum columns. The total mass of each level including the iron mass, the mass of the aluminum connections, the mass of the sensor and the mass of each half part of the support columns is m_1=15.16kg, m_2=15.16kg and m_3=12.76kg, corresponding to the 1st, 2nd and 3rd floors, respectively. The aluminum columns have 400mm of height, 120mm of width and 7mm of thickness, and are clamped at each level and at the base. The aluminum modulus of elasticity was evaluated at about 60Gpa.

Figure 9: (a) General view of the experimental setup (b) detail of the AMD

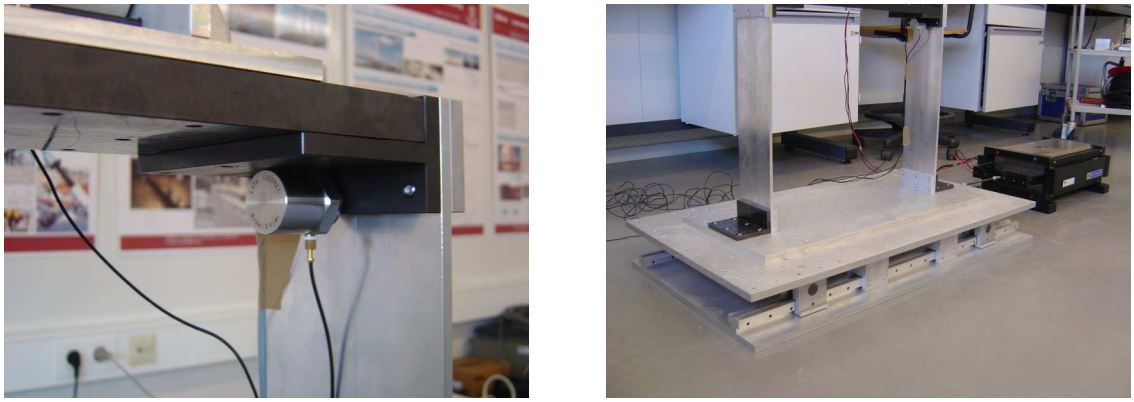

Figure 10: (a) Detail of an accelerometer (b) detail of the shaking table

In order to excite the system with harmonic loads, the physical model was fixed on a shaking table composed by a sliding platform connected to an electromagnetic shaker powered by a current amplifier (see Figure 10b). The total mass mobilized at the base of the model including the platform mass of the shaking table, the moving mass of the electromagnetic shaker, the support mass of the model, the mass of the sensor and the mass of each half part of the support columns is m_0=40.51kg.

To control vibrations in the physical model, an active mass damper was installed at the top level. This device is composed by an active 2.89kg mass, which slides with low friction through 2 circular metallic threads connected to the AMD body which has total mass of 2.65kg (see Figure 9b). The active mass is connected to a small electromagnetic shaker which is responsible to apply inertial forces between the active mass and the structure. The vein of this electromagnetic shaker has a spring of stiffness k=3840N/m causing a damped harmonic movement of the active mass when left in free vibration.

The system response was continuously measured with accelerometers positioned at the base of the model, at each floor and at the active mass of the AMD (see Figure 10a). The force developed between the active mass of the AMD and the top level was also measured with a small load cell. The current generated by the shaking table shaker and by the AMD shaker was observed too, in order to determinate the force applied with these devices.

All the transducers mentioned before, as well as the electromagnetic shakers, were operated by a digital computer using LabVIEW™ package software, helped by an acquisition board which performs the signal analog/digital conversion. A Fourier analyzer was also used in the identification of the modal parameters of the structure.

The mass and stiffness matrices of the physical model are indicated bellow, which were calculated observing the data mentioned before, and are in correspondence with the degrees-of-freedom showed in the figure. These matrices were used in the analytical calculations indicated in the next sections.

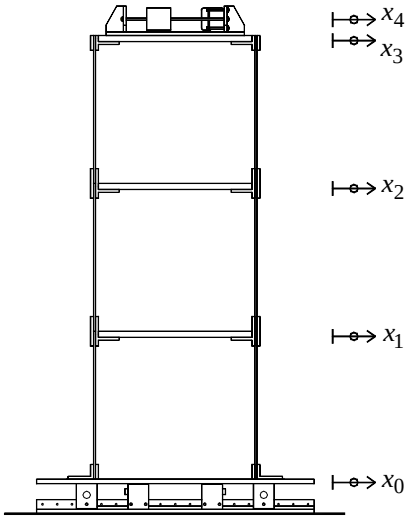

$$M = \begin{bmatrix} 40.51 & 0 & 0 & 0 & 0 \\ 0 & 15.16 & 0 & 0 & 0 \\ 0 & 0 & 15.16 & 0 & 0 \\ 0 & 0 & 0 & 15.41 & 0 \\ 0 & 0 & 0 & 0 & 2.89 \end{bmatrix} \text{kg}$$

$$K = \begin{bmatrix} 74.50 & -74.50 & 0 & 0 & 0 \\ -74.50 & 149.00 & -74.50 & 0 & 0 \\ 0 & -74.50 & 149.00 & -74.50 & 0 \\ 0 & 0 & -74.50 & 78.34 & -3.84 \\ 0 & 0 & 0 & -3.84 & 3.84 \end{bmatrix} \text{kN/m}$$

Figure 11: Identification of structure degrees-of-freedom and corresponding mass and stiffness matrices

4.2 Identification of the modal parameters of the system

In order to identify the modal properties of the system, in particular, natural frequencies, mode shapes and damping coefficients, the model was subjected to several tests and the experimental values were compared with the analytical ones obtained from the numerical model defined in the previous section (with the exception of the damping coefficients which can only be encountered via experimental results).

The natural frequencies of the system were evaluated with the help of a Fourier analyzer which allows to estimate the frequency response functions (FRFs) of a system. The FRFs are a particularization of the transfer functions of the system when the Laplace variable is substituted by $s=j\omega$. These functions characterize the system steady-state response when subjected to harmonic excitation, by giving the magnitude of the relation between output/input amplitudes and the respective phase shift.

In the case of the plane frame physical model, the FRFs can be evaluated by relating the input force applied at the base of the model by the shaking table and the output accelerations measured at the several degrees-of-freedom. For this purpose, it was stipulated a frequency range from 0 to 25Hz and it was considered the average of 5 FRFs estimates. Each FRF has an acquisition time of 16s, which means that the frequency resolution archived is 0.0625Hz.

Figure 12 shows the magnitude of the FRF obtained, relating the input force at the base of the model and the output acceleration at the top floor. The natural frequencies of the system are clearly identified by the peaks on the graph and their values, as well as the analytical ones, are listed in Table 1.

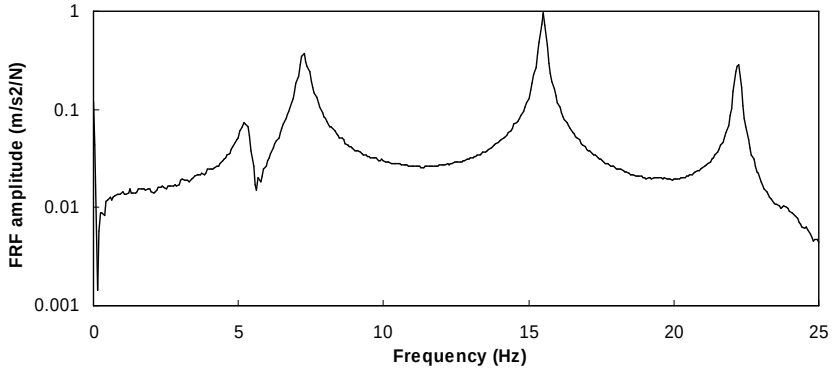

Figure 12: FRF relating the input force at the base of the model and the output acceleration at the top floor

Frequency	Identified (Hz)	Calculated (Hz)
1	5.50	5.45
2	7.35	7.35
3	15.50	14.60
4	22.50	22.25

Table 1: Identified versus analytical natural frequencies

The method used to identify the vibration mode shapes was simply exciting the structure at resonant frequencies at the base of the model using the shaking table, and measuring the amplitude and phase lag of the system response at the several degrees-of-freedom. When the structure is subject to an harmonic force with a frequency of excitation equal to a natural frequency of the system, the contribution of the other vibration modes are negligible when compared with the resonant mode.

Figure 13 shows the graphical representation of the mode shapes in correspondence with the natural frequencies indicated in Table 1. It can be observed a good agreement between the identified and calculated mode shapes in the same manner that it was observed with the natural frequencies. This means that the analytical model represents accurately the system properties in terms of mass and stiffness.

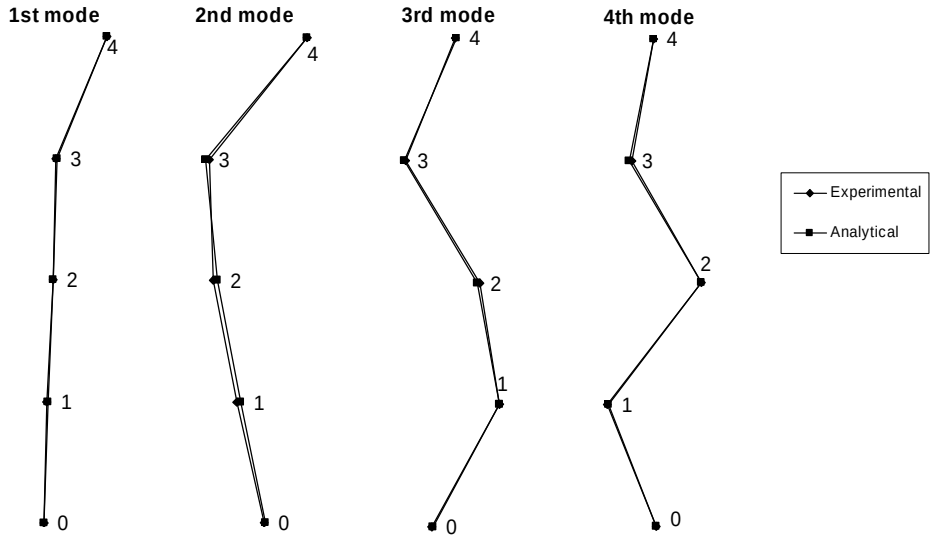

Figure 13: Identified versus analytical mode shapes

To characterize completely the system parameters it was necessary to evaluate the damping properties of the system. One way to do this consist in exciting the physical model with an harmonic force of frequency equal to any of those that were identified as a natural frequency of the system. By suddenly stopping the excitation, it is possible to measure the free vibration response and estimate the respective damping coefficient, by analyzing the free decay response envelope, given by the equation[1] $y = Ae^{-\zeta\omega t}$, where A is a real positive constant.

This procedure was adopted to estimate the modal damping coefficients of the several vibration modes of the physical model. The results obtained are showed in Figure 14, in terms of the graphical representation of the system response at the indicated degree-of-freedom, as well as the equation of the respective free decay envelope.

The study of this equation, applied to different sets of time intervals, allows to conclude that the modal damping coefficients vary slightly with the displacements

amplitude. For this reason, their values were estimated in an intermediate range of the structure response, corresponding approximately to a mean value of the damping coefficient. Table 2 summarizes the results obtained in correspondence with the different vibrations modes.

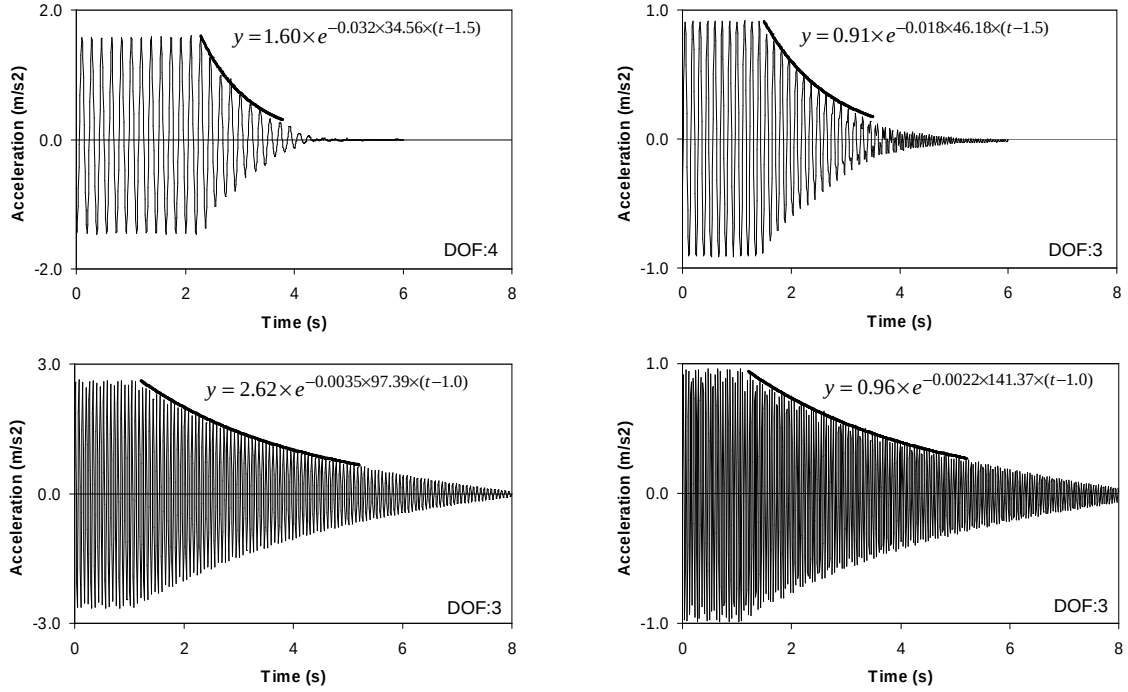

Figure 14: Free vibration responses and the estimated decay envelopes

Mode	Identified frequency (Hz)	Modal damping coefficient (%)
1	5.50	3.20
2	7.35	1.80
3	15.50	0.35
4	22.50	0.22

Table 2: Identified modal damping coefficients

Based on the modal damping coefficients evaluation, it is possible to define the damping matrix of the system using the superposition of modal damping matrices[1], resulting

$$C = \begin{bmatrix} 35.30 & -3.74 & -11.47 & -16.11 & -3.99 \\ -3.74 & 7.82 & -0.94 & -1.91 & -1.23 \\ -11.47 & -0.94 & 10.23 & 2.91 & -0.73 \\ -16.11 & -1.91 & 2.91 & 15.00 & 0.11 \\ -3.99 & -1.23 & -0.73 & 0.11 & 5.85 \end{bmatrix} \text{ kg/s}$$

5 IMPLEMENTATION OF THE CONTROL SYSTEM

5.1 Description of the control system

The objective of the control system is to reduce the vibration levels of the physical model, when it is excited with harmonic loads. When the frequency of excitation is equal to any of the natural frequencies of the structure, i.e., when resonance occurs, the system may experiment large amplitude motion, depending on the damping coefficient of the respective vibration mode. Therefore, an appropriate control strategy should be able to manipulate the damping in the system, causing a significant reduction in the structural response.

When resonance occurs, the amplitude of the dynamic system response is obtained by multiplying the static response by $1/2\zeta$, which suggests that, if the static response is known, the damping coefficient should be chosen in order to keep the dynamic response bellow certain pre-defined limits.

As seen before, the modification of the characteristics of the structure in terms of the modal damping coefficients can be obtained using an active mass damper commanded by a derivate controller. The definition of the control gains can be studied using the root-locus method which also allows to evaluate the system stability.

An important issue that must be initially considered is the location of the actuator system. The main rule is that the actuator should not be positioned at a point where the significant vibrating modes have reduced modal components.

Using the control scheme just described, a real control system was implemented in the plane frame physical model, composed by an AMD positioned at the top floor, to reduce the vibrations caused by an harmonic excitation applied by the shaking table. The system response at the top floor is continuously measured using an accelerometer connected to a signal conditioner, which performs the conversion of the accelerations into velocities by integrating the signal of the transducer. At each time instant, the control force is calculated by multiplying the value of the velocity by a pre-defined gain g, and applied to the structure by the AMD shaker connected to the respective current amplifier.

The block diagram of this close-loop control system is represented in Figure 15. The transfer function $G(s)$ was obtained directly from the system characteristics described in previous section, relating the system input/output at the top floor (DOF no.3).

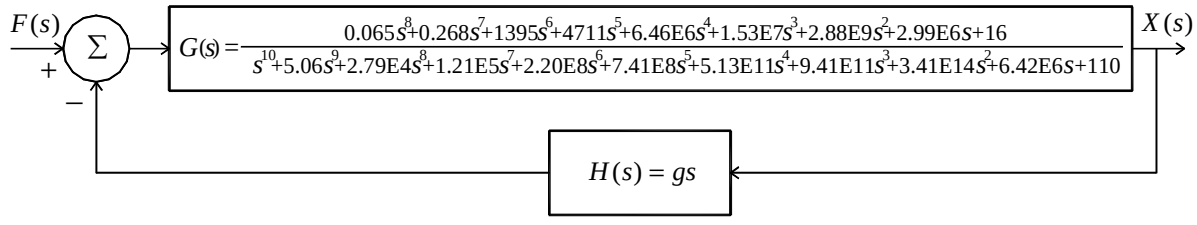

Figure 15: Block diagram of the closed-loop control system

5.2 Root-locus design

The root-locus diagram of this control system is represented in Figure 16. This plot shows clearly the advantages of this powerful method, because even if no previous information were available, looking at this diagram it is possible to immediately conclude that (*i*) the system has four natural frequencies slightly damped because the open-loop poles are close to the imaginary axis; (*ii*) the system is unstable for high gains because in this situation there are close-loop poles in the unstable region; (*iii*) there is a small gain margin until instability is reached because the AMD has relatively low damping; (*iv*) when gain increases from zero, the damping coefficients of the vibration modes also increase, despite the natural frequencies remain approximately the same.

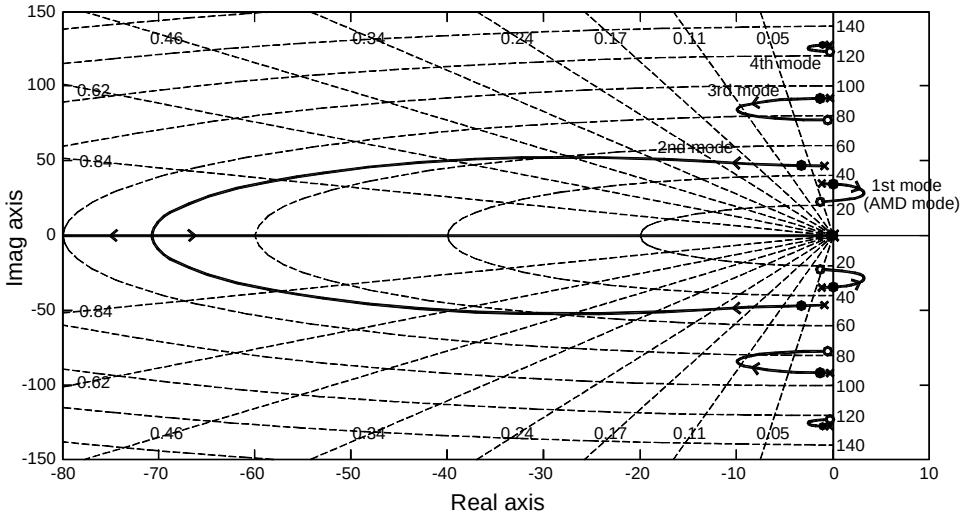

Figure 16: Root-locus diagram of plane frame controlled by an AMD

The choice of the control gain affects simultaneously all the close-loop poles locations, which means that it is not possible to select the characteristics of each vibration mode individually. For this reason, when root-locus method is used, it must be selected the dominant close-loop pole as the one that contributes more significantly to the system response. The gain is adjusted to move this pole to a more convenient position, conditioning the locations of the other poles. In the case of the present plane frame physical model, when the gain increases, all the modal damping coefficients increase in correspondence with a specific gain value, which is fixed when the target close-loop pole reaches the desired location in correspondence with a pre-defined damping coefficient.

As said before, the AMD developed for this experience has relatively low damping ($\zeta_{TMD}\approx 3.2\%$) due to construction issues, which limits the efficiency of this control system. However, even in this case it is possible to significantly increase the damping coefficients of the structure to maximum values according to the maximum achievable gain g=82, until instability occurs. If this gain is selected, the close-loop poles move to the locations marked with small dots in the root-locus diagram, which are in correspondence with the new damping coefficients listed in Table 3.

Mode	ζ_i (%) for g=0 (without control)	ζ_i (%) for g=82 (control with g_{max})
1	3.20	-
2	1.80	7.09
3	0.35	1.44
4	0.22	0.44

Table 3: Calculated modal damping coefficients for control gains g=0 and g=g_{max}=82

5.3 Experimental results

In order to experimentally verify the efficiency of the described control system, the damping coefficients of the physical model were evaluated after switching on the AMD with an intermediate gain g=60. In these circumstances, the model was excited with an harmonic load with a frequency in correspondence with the identified natural frequencies of the system and, after stopping the excitation, the free decay response was recorded in order to evaluate the respective modal damping coefficient. The results obtained are represented in Figure 17 and are summarized in Table 4, where the experimental values are also compared with the analytical ones.

System instability was also verified when the control gain exceeds its maximum value, by introducing a clearly unstable gain g=150. As expected, the noise in the sensors was sufficient to excite the system which became unstable by the uncontrolled harmonic vibration of the structure with the frequency of the AMD vibration mode. This situation is clearly predicted by the analysis of the root-locus diagram plotted in Figure 16.

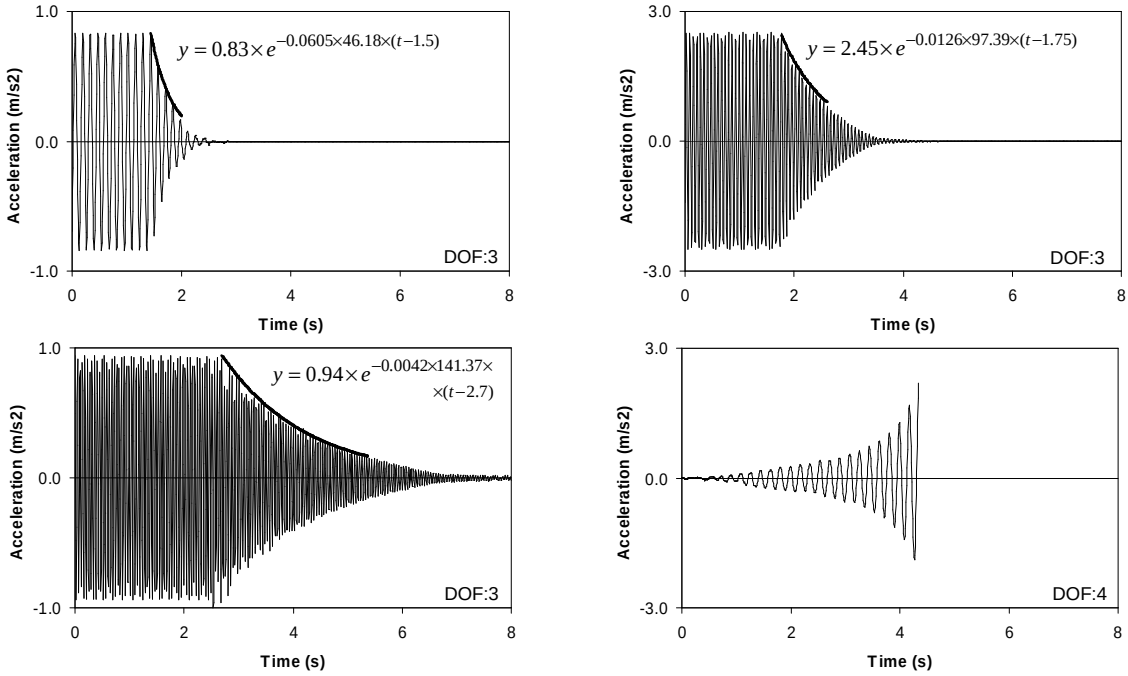

Figure 17: Free vibration responses and the estimated decay envelopes for a control gain g=60 and system response for a unstable control gain g=150

Mode	Identified (%)	Calculated (%)
1	-	0.83
2	6.05	5.72
3	1.26	1.15
4	0.42	0.38

Table 4: Identified versus calculated modal damping coefficients for a control gain g=60

6 CONLUSIONS

This document describes a laboratorial implementation of an active damping system to reduce vibrations in a 3-DOF physical model subjected to harmonic vibrations. When resonance occurs, the amplitude of the structural dynamic response is strongly influenced by the damping coefficient of the respective vibration mode. This means that a good control strategy should be able to increase the damping in the system in order to keep its response below certain limits.

For this purpose, it can be used an AMD commanded by a Derivate controller, resulting in a control system that applies an inertial force proportional to the velocity at the control point. However, the use of an AMD constitutes a non-collocated sensor/actuator scheme, causing system instability particularly for high gains. The root-locus diagram is a powerful method that allows analyzing the system stability as well as designing the control gain necessary to reach some structural properties, particularly in terms of damping coefficients.

In order to experimentally verify the efficiency of this control system, the physical model was subjected to resonant harmonic loads applied by a shaking table, and the several modal damping coefficients were evaluated by analyzing the respective free decay envelopes. It was observed a good agreement between experimental and analytical results corresponding to a significant increase of the damping ratios of the system with a consequent important reduction on its harmonic response.

ACKNOWLEDGEMENTS

The authors acknowledge the support provided by the Portuguese Foundation for Science and Technology (FCT) in the context of the research project “Control of vibrations in Civil Engineering structures”.

REFERENCES

[1] A.Chopra, *Dynamics of structures-Theory and app. earthquake eng.*,Prentice-Hall (1995)
[2] A. Preumont, *Vibration control of active structures*, Kluwer Academic Publishers (1997)
[3] H. Vu and R.Esfandiari, *Dynamic systems – Modeling and analysis*, McGraw-Hill (1998)
[4] K. Ogata, *Modern control engineering*, Prentice-Hall (1996)
[5] L. Hanagan and M. Murray, *Active control approach for reducing floor vibrations*, Journal of structural engineering, pp.1497-1505 (1997)